Dynamics of Continuous, Discrete and Impulsive Systems
Series **B:** *Applications & Algorithms* **14 (S8) (2007)** 91-102
 http://www.watam.org

LARGE-SCALE STRUCTURES SUPPRESSION IN A PLANE JET USING HIGH-FREQUENCY PERTURBATIONS

H. J. Zhang,[1] Y. Zhou[2] and L. Cheng[2]

[1]College of Metrological Technology and Engineering
China Institute of Metrology, Hangzhou, 310018, P. R. China
[2]Department of Mechanical Engineering
The Hong Kong Polytechnic University, Hong Kong SAR, P. R. China

Abstract. Piezo-ceramic actuators were used to control the large-scale vortical structures in a plane jet. The actuators were embedded into the lower lip of a slot nozzle to drive a thin plate to perturb the initial jet flow in the vertical direction. Experiments were carried out at $Re = 4000 - 6670$, and the normalized excitation frequency (St_e) was set at about 0.75, which is much higher than the preferred mode frequency. The flow fields were visualized and measured using particle image velocimetry (PIV). The velocity fluctuations were measured using an X-wire probe at $x/H = 2 - 10$. The PIV-measured flow images indicate that the large-scale structures in the jet were considerately suppressed in size once the perturbation was introduced. The observation is supported by the reduced $\overline{u^2}$ and $\overline{v^2}$, and also the spectral analysis of the fluctuating velocity. For instance, at $y/H \approx -0.7$, $x/H = 6$, at $Re = 6670$, $\overline{u^2}$ and $\overline{v^2}$ of the perturbed jet dropped by 18%, compared with the natural jet; meanwhile, the pronounced peak in the $u-$ or $v-$ spectrum retreated significantly.
Keywords. Plane jet, Piezo-ceramic actuator, Large-scale structure, Active flow control, High frequency perturbation.
AMS (MOS) subject classification:

1 Introduction

Large-scale coherent structures are one of the intrinsic features of turbulent mixing layers and jets [1-4]. The presence of these structures in a jet can cause hydrodynamic instabilities in the combustor applications, which are harmful in most of the cases and therefore undesirable [5]. To suppress coherent structures or to obtain the desired performance, a great deal of efforts has been made in jet control, which can be either passive or active [6-8]. Previous investigations [9-11] have indicated that a small disturbance at the initial boundary layer could alter the entire jet, especially the coherent structures. Therefore, active flow control is usually performed at the exit of a jet nozzle with perturbations generated by sound source or MEMS-based actuators [12, 13].

For local excitations, the excitation direction, i.e. the streamwise or the lateral direction, may have a considerable effect on the control performance. Excitations are usually applied in the lateral direction probably because the lateral direction excitation is easy to manipulate and effective to control the flow behaviors. For example, Lepicovsky [14] suggested that an increase in vertical velocity fluctuations in the shear layer enhances the vortex formation and hance mixing. Recently, Suzuki et al. [7] mounted flap actuators on the periphery of a circular nozzle exit, which were driven vertically to induce various flow modes and to enhance mixing processes. They found that the flap actuators could significantly modify the large-scale vortical structures. Similar method has been used on a coaxial jet nozzle to control fuel-air mixing and diffusion combustion [15,16]. It was observed that shedding of large-scale vortex rings are modified with the flap motion, and the flame characteristics are successfully manipulated. Attempt was also made to perturb a jet in the streamwise direction. Wiltse and Glezaer [17] used piezoelectric actuators for flow control in a jet emanating from a square conduit. In their work, the mixing layer was perturbed in the streamwise direction using a high frequency carrier, and the actuators were positioned at a short distance downstream of the jet exit plane.

This paper presents a different approach using open-loop-controlled piezoceramic actuators installed at the exit of the nozzle. The essence of the technique is to create a local perturbation in the nozzle exit surface, which subsequently alters the entire flow field, in particular, suppressing large-scale structures using a perturbation frequency which is about three times that of the dominant structures.

2 Experiment Details

Experiments were carried out using a $300 \times 20mm$ plane jet facility. Air was supplied by a centrifugal blower. Air was blown into a settling chamber, passing through a series of screens and honey combs before entering the nozzle contraction section, whose contraction ratio was 15 (Fig. 1a). The upper and lower plates of 40mm long in the x-direction served as the nozzle upper and lower lips. See Fig.1a for the definition of the coordinate system. Two end plates ($250 \times 200mm$) were used to ensure the two dimensionality of the plane jet up to $x/H = 12$, where x is the downstream distance from the nozzle exit, and $H(= 20mm)$ is the nozzle height. The lower plate had a slot, in which an actuator holder was installed (Fig. 1b). Two THUNDER (Thin layer composite UNimorph piezoelectric Driver and sEnsoR) actuators were fixed on the holder at one end, with the other end connected to a thin plastic plate of 3mm thick. The THUNDER actuators were developed by the NASA Langley Research Center. This actuator has been used for vibration isolation, aeroelastic response control, airfoil shaping and vortex induced vibration control [18]. The upper surface of the plate was flush with the lower lip surface of the nozzle by adjusting the position of the actuator holder. Driven by the actuators, this plastic plate could oscillate at amplitude of Y_e up to 1.2mm, creating a local perturbation to flow. The actuating signal was generated by a signal generator and amplified by a dual-channel piezo driver amplifier (Trek PZD 700). A Dantec standard PIV2100 system was used to measure the flow field. The flow was illuminated in the x-y plane of about 2-3mm in thickness by double-pulsed Yag laser (NewWave) at a wavelength of 532 nm. The PIV images were captured by a CCD camera (HiSense type 13, 1280 $\times$ 1024 pixels). Each image covered a view area typically of 132 mm $\times$ 119mm, i.e. $x/H \approx 1.0 \sim 7.6$ and $y/H \approx -3 \sim +3$. Instantaneous velocities of the jet were acquired at the flow centerline using a $5\mu m$ tungsten X-wire probe, and the cross-flow distributions of velocities were also measured at $x/H = 2$,

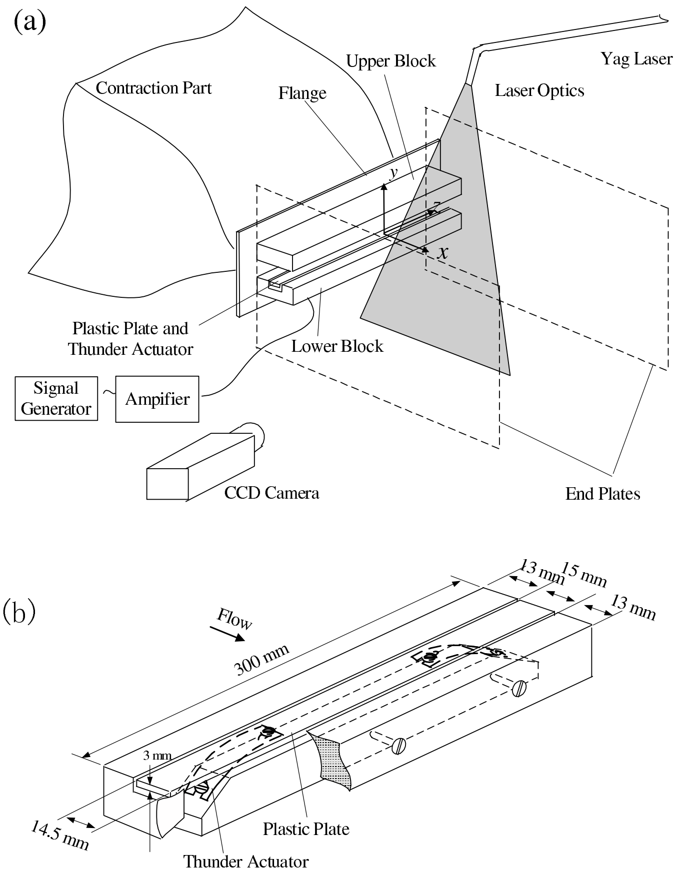

Figure 1: Experimental setup: (a) the nozzle and the PIV system; (b) the installation of actuators.

6 and 10 downstream of the nozzle exit. Measurements, with and without flow control, were made at the jet exit velocity (U_j) of 3-5m/s, corresponding to the Reynolds numbers Re ($\equiv U_j H/\nu$, where ν is the kinematic viscosity of air) of 4000 - 6670.

The excitation frequency often plays a crucial role in the jet control. To determine the frequencies that should be used, a preliminary test was performed. The excitation frequency was varied from 0 to 200/230 Hz (for Re = 4000/6670) under a constant activating voltage of 110V, while the X-wire probe, located in the shear layer at $x/H = 6$, recorded the velocity fluctuations, u and v, in the x and y directions, respectively. The test results were shown in Fig. 2. For the excitation frequency $f_e = 60 \sim 160Hz$ at $Re = 4000$ and $f_e > 40Hz$ at $Re = 6670$, the velocity fluctuation variances, $\overline{u^2}$ and $\overline{v^2}$, of the perturbed jets are smaller in magnitude than their counterparts of a natural jet, suggesting weakened coherent structures. At $f_e = 120Hz$ for $Re = 4000$ and $f_e = 190Hz$ for $Re = 6670$, both $\overline{u^2}$ and $\overline{v^2}$ reach their lowest values. Therefore, the excitation frequencies $f_e = 120Hz$ or $St_e(\equiv f_e H/U_j) = 0.8$, and $f_e = 190Hz$, or $St_e = 0.75$ were chosen for the two Reynolds numbers to examine the effectiveness of the excitations. The natural jet was also measured for comparison.

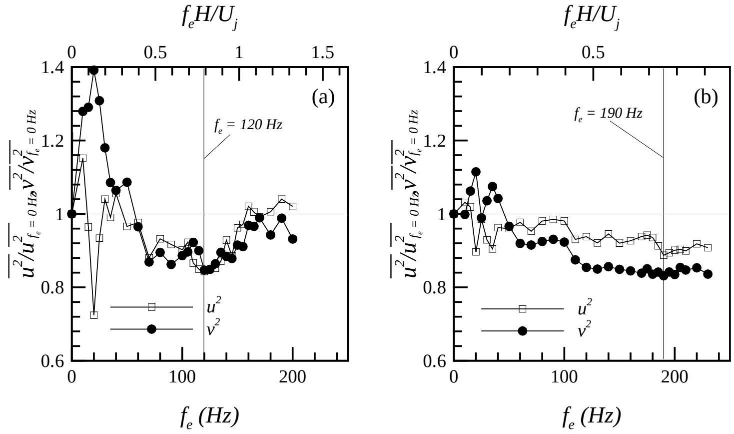

Figure 2: Dependence of the controlled velocity variances on the perturbation frequency. A constant voltage 110 V was applied. The X-wire probe was located at $x/H = 6, y/H = -1$. (a) $Re = 4000$, (b) $Re = 6670$.

3 Results and Discussions

3.1 Flow patterns

Similarly to previous studies [1,19], the preferred mode of the flow structures was found in the present jet, as indicated by a dominant peak in the v-spectrum (not shown here). The normalized frequency of the preferred mode $St_p(\equiv f_pH/U_j)$, where f_P is the frequency of the preferred mode) is about 0.26 for both Reynolds numbers, i.e., about one third of St_e for both cases. Figures 3 and 4 present typical photographs from flow visualization, where the flow is left to right. The large-scale organized structures are evident at Re = 4000 and appear to be laminar in the immediate vicinity of the nozzle in the absence of the perturbation (Fig. 3a). While the symmetrical

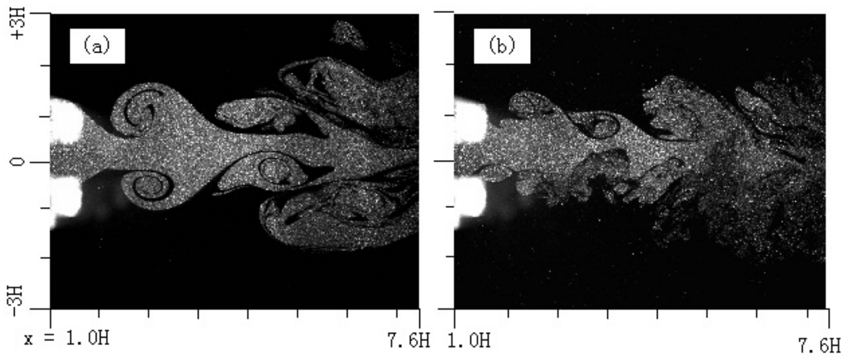

Figure 3: Typical flow patterns at $Re = 4000$: (a) Natural jet, (b) Perturbed jet.

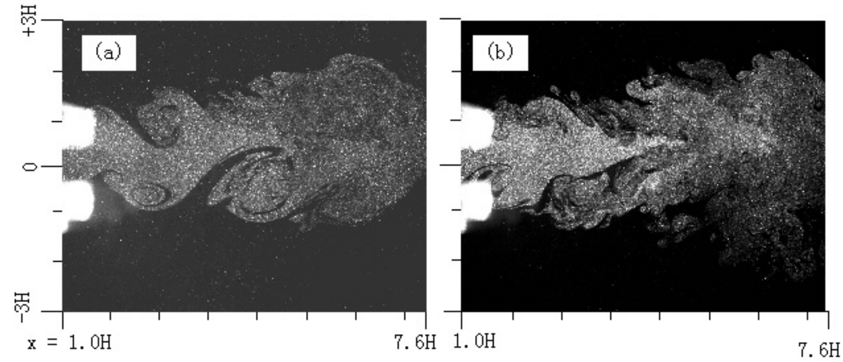

Figure 4: Typical flow patterns at $Re = 6670$: (a) Natural jet, (b) Perturbed jet.

vortical structures occur in the natural jet (Fig. 3a), anti-symmetric patterns were also observed (not shown here). As the perturbation was applied, the organized structures (Fig. 3b) now appear to be turbulent and rather small in size. At Re = 6670 (Fig. 4), the organized structures start rolling up at the nozzle lips in the natural jet (Fig. 4a). As the jet was excited, as illustrated in Fig. 4b, large-scale organized structures could not be seen in the near field, only smaller eddies being evident instead.

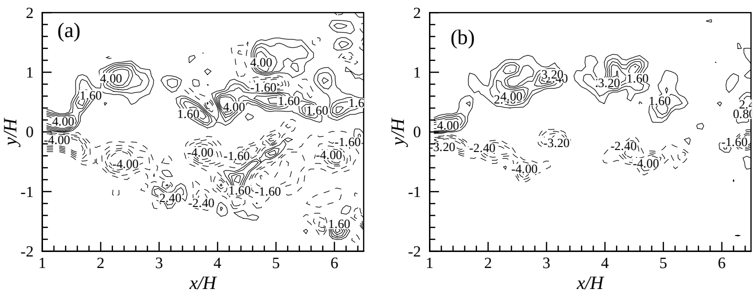

Figure 5: The iso-contour of spanwise vorticity $\omega^* = \omega H/U_j$ from the PIV measurements: (a) Natural jet, (b) Perturbed jet. (Contour interval = 0.8, $Re = 4000$).

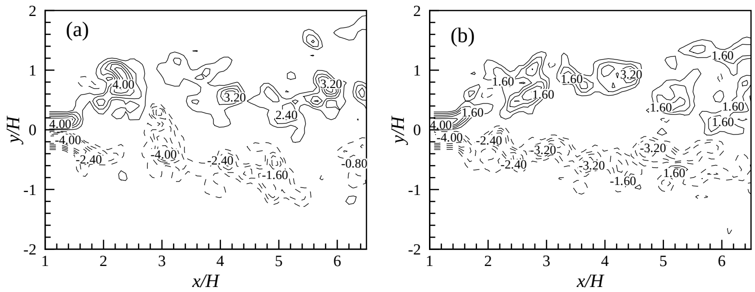

Figure 6: The iso-contour of spanwise vorticity $\omega^* = \omega H/U_j$ from the PIV measurements: (a) Natural jet, (b) Perturbed jet. (Contour interval = 0.8, $Re = 6670$).

The iso-contours (Figs. 5 and 6) of the PIV-measured vorticity, , provide the quantitative information of the jets with and without perturbation. Since the contour level is the same for both natural and perturbed jets, the size of the contour of the same level may represent the vortex scale. For the natural jet, at $Re = 4000$ (Fig. 5a), a large-scale concentration of negative sign was found at $x/H \approx 2.5$ and $y/H \approx -0.5$, implying a negative vortex. At the same time, a positive vortex, although less organized, is present at $x/H \approx 2.5$

and $y/H \approx 0.5$, symmetrical about the flow centerline with respect to the negative one. At $Re = 6670$ (Fig. 6a), vortices became anti-symmetrical about the flow centerline. While for the perturbed jet (Figs. 5b and 6b), the large-scale vortices were replaced by the relatively small-scale eddies. The observations suggest that the size and strength of the large-scale structures have been significantly reduced as a result of the perturbation, conforming to the results of flow visualization.

3.2 Mean and fluctuation velocity profiles

Figures 7 and 8 show the cross-flow distributions of mean velocity and Reynolds stresses at $x/H = 2$, 6 and 10, under different conditions: without perturbation (a natural jet) and with the perturbations at $Re = 4000$ and 6670, respectively. It was found that for both of Reynolds number cases the mean velocity and the Reynolds shear stress were insensitive to the control and the same observations were made for Reynolds normal stresses.

At $x/H = 2$, the perturbed and appear greater than their counter parts of the natural jet (Figs. 7(a-2,3), 8(a-2,3)), especially at $y/H < 0$, but become smaller than those of the natural jets at $x/H = 6$ and 10 (Figs. 7(b-2,3), 7(c-2,3), 8(b-2,3) and 8(c-2,3)). The perturbation leads to a considerable reduction in and at $y/H = -1 \sim +1$, up to 16% for $Re = 4000$ and 18% for $Re = 6670$ at $x/H = 6$ and $y/H \approx -0.7$. The smaller and suggest the reduced size of the large-scale structures.

3.3 Spectral analysis

Insight into the control effects on the jet may be obtained from the power spectral density functions, E_u and E_v (Figs. 9 and 10), of the streamwise and lateral velocities measured at $y/H = -0.5$, -1 and -1 for $x/H = 2$, 6 and 10, where large scale structures pass over (Refer to Figs. 7 and 8). At $x/H = 2$, peaks at the perturbation frequency or its harmonics are prominent (Figs. 9a and 10a). These peaks disappear further downstream at x/H = 6 and 10 (Figs. 9b,c and 10b,c). At $x/H = 6$ and 10, the prominent peak does not occur at the preferred frequency, but at its sub-harmonics. This is because the large-scale structures coalesce as moving downstream. As expected, at $x/H = 6$ (Figs. 9b and 10b), E_u and E_v in the perturbed jet show a considerable less pronounced peak than the natural jet, indicating that the high-frequency perturbation has weakened large-scale structures in the jet. At $x/H = 10$ (Figs. 9c and 10c), the peaks become broader, suggesting less organized coherent structures. Again, the perturbed jet displays a lower peak than the natural jet, indicating that the perturbation still effective.

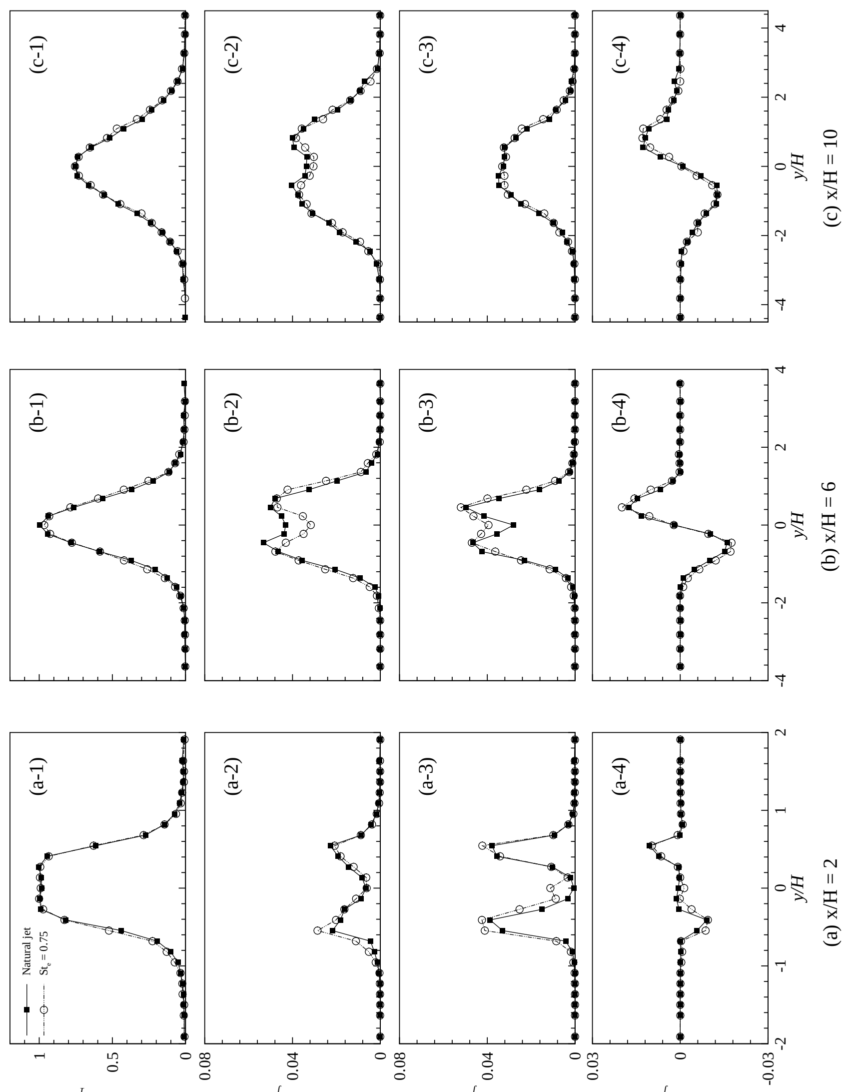

Figure 7: Lateral distributions of mean velocity $\overline{U}$, Reynolds stresses $\overline{u^2}$ and $\overline{v^2}$ and $\overline{uv}$ at a$x/H = 2$, (b) 6, (c) 10. ($Re = 4000$).

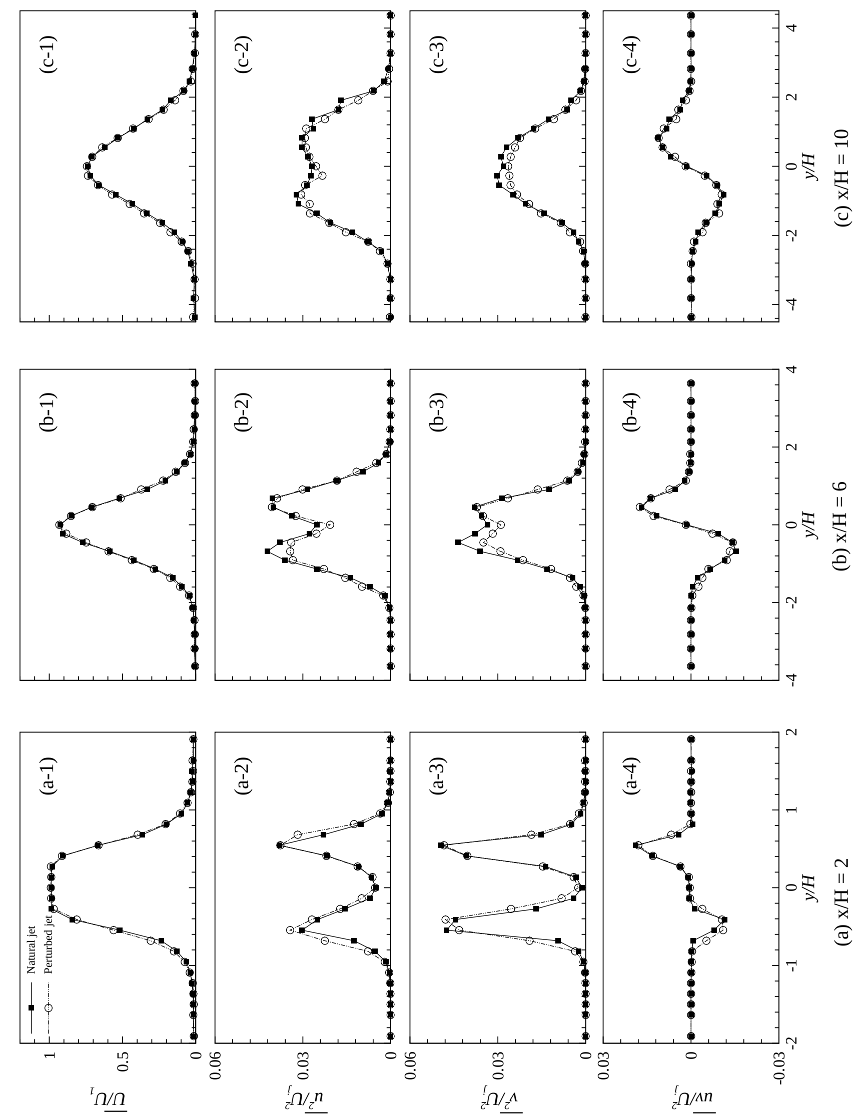

Figure 8: Lateral distributions of mean velocity $\overline{U}$, Reynolds stresses $\overline{u^2}$ and $\overline{v^2}$ and $\overline{uv}$ at a$x/H = 2$, (b) 6, (c) 10. ($Re = 6670$).

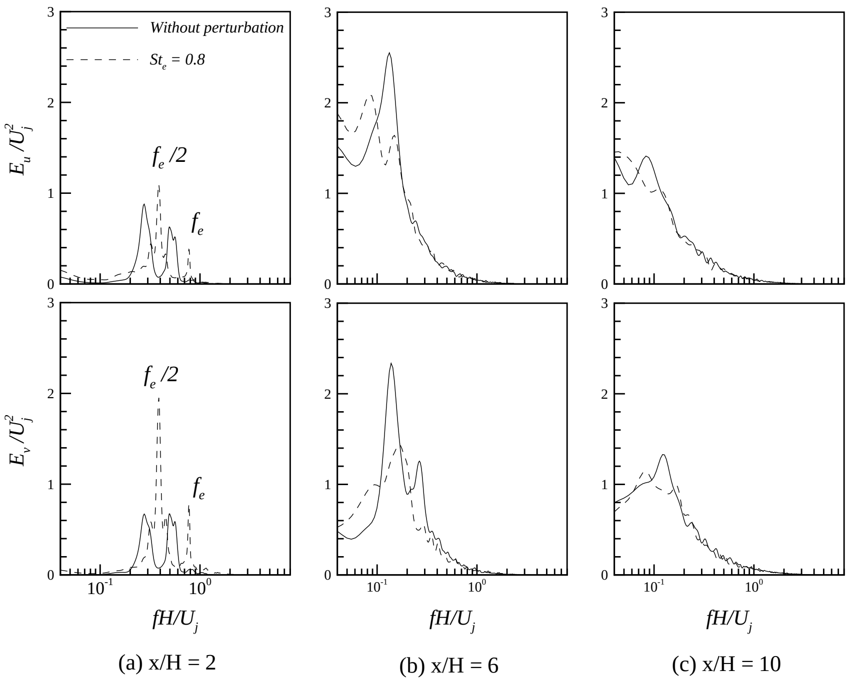

Figure 9: Power spectral density functions, E_u and E_v, of the streamwise and lateral velocities for the natural and perturbed jet with $St_e = 0.8$ at $Re = 4000$: (a) $x/H = 2$, (b) 6, (c) 10. Hotwire probe was placed at (a) $y/H = -0.5$; (b) -1; (c) -1.

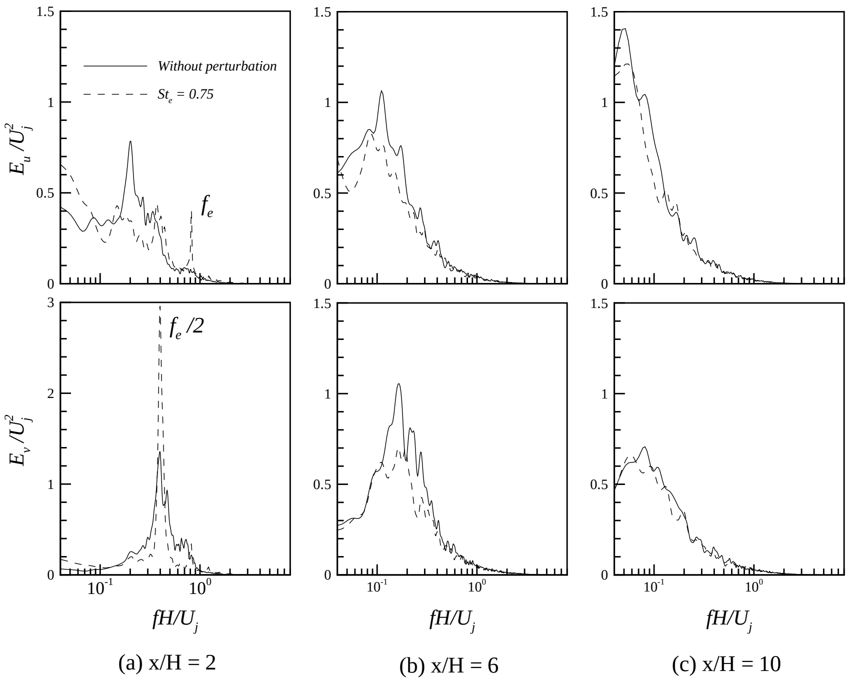

Figure 10: Power spectral density functions, E_u and E_v, of the streamwise and lateral velocities for the natural and perturbed jet with $St_e = 0.75$ at $Re = 6670$: (a) $x/H = 2$, (b) 6, (c) 10. Hotwire probe was placed at (a) $y/H = -0.5$; (b) -1; (c) -1.

4 Conclusions

Piezo-ceramic actuators were used in the open-loop control of a plane jet. The PIV data and visualization photos show that in the perturbed jet, the size and the strength of the large-scale structures decreased. The mean velocity and Reynolds shear stress distributions of the perturbed jet were similar to their counterpart in an unperturbed jet. However, the velocity fluctuations, $\overline{u^2}$ and $\overline{v^2}$, were significantly reduced, for example, $\overline{u^2}$ and $\overline{v^2}$ of the perturbed jet at $Re = 6670$ dropped by 18%, compared with the natural jet. This implies that the large-scale structures in the flow have been weakened. Power spectral density functions of velocity fluctuations shown that the peaks at the preferred mode frequency or its harmonics are less pronounced in the perturbed jet than in the natural jet, indicating less organized coherent structures. The investigation indicates that the present control technique is effective in impairing the coherent structures.

5 Acknowledgements

This work is partially supported by the Scientific Research Foundation for the Returned Overseas Chinese Scholars, State Education Ministry, and supported by Zhejiang Province Natural Science Fundation (Y604559), P. R. China. The authors wish to acknowledge financial support given to them by the Research Grants Council of the Government of the HKSAR through grants PolyU 5316/03E and PolyU 1/02C.

6 References

[1] S. C. Crow and F. H. Champagne, Orderly structure in jet turbulence, *J. Fluid Mech.*, **48**, (1971), 547-591.

[2] G. L. Brown and A. Roshko, Density effects and large structure in turbulent mixing layers, *J. Fluid Mech.*, **64**, (1974), 775-816.

[3] C. M. Ho and P. Huerre, Perturbed free shear layers, *Ann. Rev. Fluid Mech.*, **16**, (1984), 365-424.

[4] B. J. Cantwell, Organized motion in turbulent flow, *Ann. Rev. Fluid Mech.*, **13**, (1981), 457-515.

[5] K. R. McManus, T. Poinsot and S. M. Candel, A review of active control of combustion instabilities, *Prog. Energy Combust. Sci.*, **19**, (1993), 1-29.

[6] J. F. Olsen, S. Rajagopalan and R. A. Antonia, Jet column modes in both a plane jet and a passively modified plane jet subject to acoustic excitation, *Experiments in Fluids*, **35**, (2003), 278-287.

[7] H. Suzuki, N. Kasagi and Y. Suzuki, Active control of an axisymmetric jet with distributed electromagnetic flap actuator, *Experiments in Fluids*, **36**, (2004), 498-509.

[8] F. O. Thomas and V. W. Goldschmidt, Acoustically induced enhancement of widening and fluctuation intensity in a two-dimensional turbulent jet, *J. Fluids Engineering*, **108**, (1986), 331-337.

[9] C. Tong and Z. Warhaft, Turbulence suppression in a jet by means of a fine ring, *Physics of Fluids*, **6**(1), (1994), 328-333.

[10] P. Burattini, R. A. Antonia, S. Rajagopalan and M. Stephens, Effect of initial conditions on the near-field development of a round jet, *Experiments in Fluids*, **37**, (2004), 56-64.

[11] K. B. M. Q. Zaman and A. K. M. F. Hussain, Turbulence suppression in free shear flows by controlled excitation, *J. Fluid Mech.*, **103**, (1981), 133-159.

[12] V. Faivre and T. Poinsot, Experimental and numerical investigations of jet active control for combustion applications, *Journal of Turbulence*, **5**, (2004), paper no. 25.

[13] J. M. Wiltse and A. Glezer, Manipulation of free shear flows using piezoelectric actuators, *J. Fluid Mech.*, **249**, (1993), 261-285.

[14] J. Lepicovsky, The role of nozzle exit boundary layer velocity gradient in mixing enhancement of free jets, *Proceedings of the Third Joint ASCE/ASME Mechanics Conference*, La Jolla, CA, July 9-12, 1989, 41-47.

[15] N. Kurimoto, Y. Suzuki and N. Kasagi, Active control of lifted diffusion flames with arrayed micro actuators, *Experiments in Fluids*, **39** (6), (2005), 995 - 1008.

[16] N. Kasagi, Toward smart control of turbulent jet mixing and combustion, *International Conference on Jets, Wakes and Separated Flow*, October 5-8, 2005, Toba-shi, Mie, Japan.

[17] J. M. Wiltse and A. Glezer, Direct excitation of small-scale motions in free shear flows, *Physics of Fluids*, **10** (8), 1998, 2026-2036.

[18] L. Cheng, Y. Zhou and M. M. Zhang, Perturbed interaction between vortex shedding and induced vibration, *Journal of Fluids and Structures*, **17**, (2003), 887-901.

[19] R. A. Petersen and M. M. Samet, On the preferred mode of jet instability, *J. Fluid Mech.*, **194**, (1988), 153-173.

email:journal@monotone.uwaterloo.ca
http://monotone.uwaterloo.ca/∼journal/